High Responsivity and Gate Tunable Graphene-MoS_2 Hybrid Phototransistor

*Hua Xu, Juanxia Wu, Qingliang Feng, Nannan Mao, Chunming Wang, and Jin Zhang**

A 2D atomic-layer-thickness phototransistor based on a graphene-MoS_2 bybrid device is constructed with a photoresponse much larger than that of individual graphene or MoS_2 based phototransistors. Strong and selective light absorption in the MoS_2 layer creates electric charges that are transferred to graphene layers derived by a build-in electrical field, where they recirculate many times due to the high carrier mobility of graphene. Gate tunable Fermi level in graphene layer allows the responsivity of this hybrid phototransistor to be continuously tuned from 0 to about 10^4 mA/W by the gate voltage. Furthermore, large scale, flexible, and transparent 2D phototransistors with high responsivity are constructed from the CVD-grown graphene and MoS_2 flakes. The high responsivity, gate-tunable sensitivity, wavelength selectivity, and compatibility with current circuit technologies of this type device give it great potential for future application in integrated nano-optoelectronic systems.

1. Introduction

High responsivity photodetector is highly desired for various demanding applications, such as optical communication, imaging, and sensing.[1] Recently, photodetectors based on silicon semiconductors, organic semiconductors,[2] quantum dots[3] and carbon nanotubes[4] have been extensively studied. The two main types of photodetector are photodiodes and photoconductors.[1] Photodiodes are fast responding but have low gains that are usually less than 1. Photoconductors, in contrast, are capable of high gain because one type of charge carrier is able to circulate through an external circuit many times before it recombines with its opposite carrier. The types of photodetector are usually determined by the materials which are used in the transistor.

Two-dimensional (2D) atomic crystal, such as graphene, MoS_2, etc. has attracted great attention in recent years because of their superior electrical and optical properties and potential applications in future electronics and optoelectronics.[5–10] The 2D phototransistor represented by graphene phototransistor is becoming the focus of the research topic, and is expected to be used in next generation ultrathin and flexible optoelectronic devices.[11–13] Graphene phototransistors, which work based on the photodiode mechanism, have been used as ultra-fast photodetectors for high-speed optical communications because of their high carrier mobility.[13] However, the responsivity of the detectors is very low (≤ 6.1 mA/W) because of the weak light absorbance of graphene (≈2.3% for single layer graphene), and it is no wavelength selectivity due to the special electronic

H. Xu, J. X. Wu, Q. L. Feng, N. N. Mao, Prof. J. Zhang
Center for Nanochemistry
Beijing National Laboratory for Molecular Sciences
Key Laboratory for the Physics and Chemistry of Nanodevices
State Key Laboratory for Structural Chemistry of Unstable and Stable Species, College of Chemistry and Molecular Engineering
Peking University
Beijing 100871, P. R. China
E-mail: jinzhang@pku.edu.cn

Dr. J. X. Wu
Academy for Advanced Interdisciplinary Studies
Peking University
Beijing 100871, P. R. China

Dr. Q. L. Feng, Prof. C. M. Wang
College of Chemistry and Chemical Engineering
Lanzhou University
Lanzhou 730000, P. R. China

DOI: 10.1002/smll.201303670

© 2014 Wiley-VCH Verlag GmbH & Co. KGaA, Weinheim

small

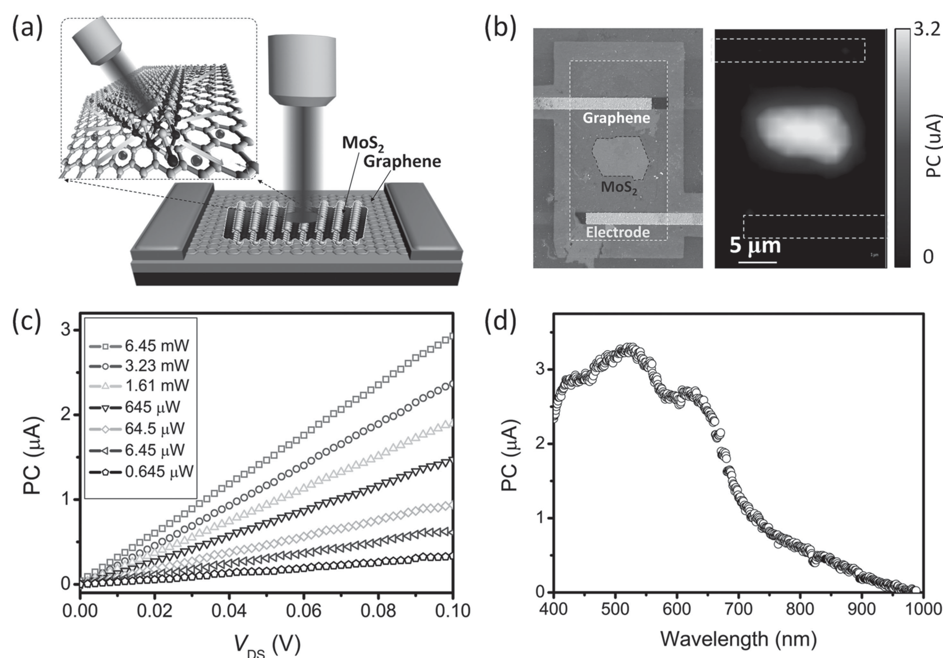

Figure 1. (a) Schematic diagram of a graphene-MoS_2 hybrid phototransistor under light irradiation. (b) SEM image and spatial photocurrent profile of the graphene-MoS_2 hybrid phototransistor. A focused laser beam at 632.8 nm with power of 6.45 mW and diameter of 2 µm was used. The photocurrent was recorded as the laser beam was scanned across the surface of the detector. (c) Photocurrent of the graphene-MoS_2 transistor for different optical power as a function of drain–source voltage (V_{DS}), showing a linear dependence on the bias voltage ($V_{BG} = 0$). The total current ($I_{dark} + I_{light}$) are shown in Figure S2. (d) Photocurrent response of the graphene-MoS_2 phototransistor as a function of the wavelength of irradiation light ($V_{DS} = 0.1$ V; $V_{BG} = 0$ V).

structure of graphene make it has a broad absorption in the whole wavelength range. Unfortunately, the zero band gap and the extremely short exciton life-time (in the ps range) of graphene make its phototransistor can't work with the photoconductor mechanism. So far, most development of graphene-based photodetection is focused on the enhancement of the absorption of light in graphene, for example by exploiting thermoelectric effects,[14] metallic plasmonics,[15] graphene plasmons[16] or microcavities.[17] Until just recently, the idea implementation of photoconductive gain — the ability to provide multiple charge carriers per single incident photon was realized by modifying the graphene transistor with quantum dots,[18–20] which was considered as the key to ultrasensitive graphene-based photodetection.[18]

Another 2D material MoS_2 has been considered as a new star for application in future electronic devices, because of its large band gap and relative high carrier mobility.[7,21] The thickness dependent band gap, the specific lattice and electronic band structure of MoS_2 also endow it many novel optical properties.[22,23] Recently, single-layer and few-layer MoS_2 phototransistor has been constructed, it shows selective photodetection capabilities to red and green light with triple, double and single layer thickness.[24–26] However, the responsivity of MoS_2 phototransistor is still low due to its low carrier mobility. Moreover, a Schottky-junction is usually formed at MoS_2/electrode interface, which will inevitably lead the photodetection capabilities to be dependent on the electrode materials.

From above we know that for graphene and MoS_2, each material has their spotlight merit, but fatal weakness, which limit their potential application in optoelectronics. In order to complement the merit and the weakness of these materials, here we construct the graphene-MoS_2 hybrid phototransistor (**Figure 1**a), using MoS_2 as sensitizer to absorb light, and graphene as an expressway for carrier transport, where the photo-excited carriers generated from MoS_2 film can be transferred to the graphene layer under the driving of a build-in electrical field. With this ingenious designing, the responsivity of the phototransistor can up to 10^4 mA/W, which is much larger than that of individual graphene or MoS_2 based-phototransistor. On the basis of deep understanding of charge transfer mechanism, the gate tunable photoresponse and the symmetric mirror-imaging photoswitching effect are realized in our device. In addition, large scale, flexible and transparent 2D graphene-MoS_2 phototransistor with high responsivity was constructed by using the CVD grown graphene and MoS_2 films. Furthermore, the understanding of the charge transfer between graphene and MoS_2 are beneficial to the study of more complex 2D atomic crystal multi-heterostructure devices,[27,28] which are widely studied recently for the potential to be used in future high performance electronics.

2. Results and Discussion

Figure 1b shows the SEM image of the graphene-MoS_2 bybrid phototransistor device (left) and the spatially resolved photocurrent response of the device on light irradiation (right), measured with a focused laser beam. Different from the graphene-based photodetectors reported previously, where photocurrent generation occurs just at the interface of

 © 2014 Wiley-VCH Verlag GmbH & Co. KGaA, Weinheim

graphene and metal electrode, or in the vicinity of a p-n junction, the photocurrent response of our device overs the whole area of the MoS_2 flake overlapping with the graphene film, a feature of importance in most sensing applications. Especially, the photocurrent is extremely large even to completely cover that at the interface of graphene and metal electrode contacts. The dependence of photocurrent response on the bias voltage applied between the source and drain electrodes (V_{DS}) is shown in Figure 1c, which reveals that the photocurrent (PC = $I_{light} - I_{dark}$) depends linearly on the V_{DS}. However, in contrast, the photocurrent arised from the thermoelectric effects at graphene p-n junction or MoS_2/metal electrode interface shows independence on the V_{DS}.[12,29] Figure 1d shows the photocurrent as a function of the wavelength of irradiation light at fixed V_{DS} = 0.1 V and zero back gate voltage (V_{BG}). Clearly, the photocurrent response spectra of our device correspond well with the absorption of the MoS_2 film measured in previous report.[26] The spectral sensitivities of the devices are determined by the absorption spectra of the MoS_2 film, and thus could be tuned easily by controlling the thickness of MoS_2 film. These results clearly demonstrate that MoS_2 film on graphene surfaces does play a key role to the photocurrent generation in our device.

Next we will reveal the responsivity of the graphene-MoS_2 phototransistor. **Figure 2**a shows the photocurrent response of our device to on-off light irradiation at different light power. The photocurrent shows decreasing tendency with the light irradiation decreasing. As shown in Figure 2b, on the other hand, the responsivity increases with the decrease of the light irradiation, which is consistent with photoconductor based sensors previously reported.[18] The curve can be fitted well with the equation $R = \alpha E^{\beta\text{-}1}$, which was successfully used for phototransistor based on graphene and PbS based device before.[20] Remarkable, the responsivity of the device can up to about 1×10^4 mA/W with an incident power of 0.645 µW at (V_{DS} = 0.1 V, V_{BG} = 0 V), which is several orders of magnitude higher than that of the MoS_2 phototransistor (7.5 mA/W at V_{DS} = 1 V and V_{BG} = 50 V) and graphene phototransistor (6.1 mA/W) previously reported.[13,25] It is notable that the photocurrent response of the detector is still very large (0.7 µA) even at the smaller V_{DS} (0.1 V) and the weakest light irradiation (0.645 µW). Restricted by the instrument we haven't measured the responsivity at even lower light irradiation, but we believe that it should be even larger than the value we measured here at a larger V_{DS} value or a lower light power irradiation (such as to the order of nW or pW). Furthermore, the on-off photoswitching effect of this phototransistor is quite fast (Figure 1c). The photocurrent sharply increased to the saturation within ≈0.28 s of exposure when MoS_2 film reached the maximum of photo-excited charge separation. On the contrary, after the high conductance state was established and the device was kept in the dark, the device presented a fast current relaxation, completing the decrease after ≈1.5 s. This can be explained as the fast charge recombination of the holes in conductive graphene channel by the electrons in the MoS_2 films.

To get a better understanding of the sensing mechanism, we characterized the transfer characteristics of the graphene-MoS_2 device under dark and light irradiation with different irradiation power. To eliminate the effect of gate hysteresis on our results, we used a device prepared from mechanical exfoliated graphene (see Figure S1 (c and d)) to perform the experiment. As shown in **Figure3**a, the resistance as a function of backgate voltage (V_{BG}) under different light

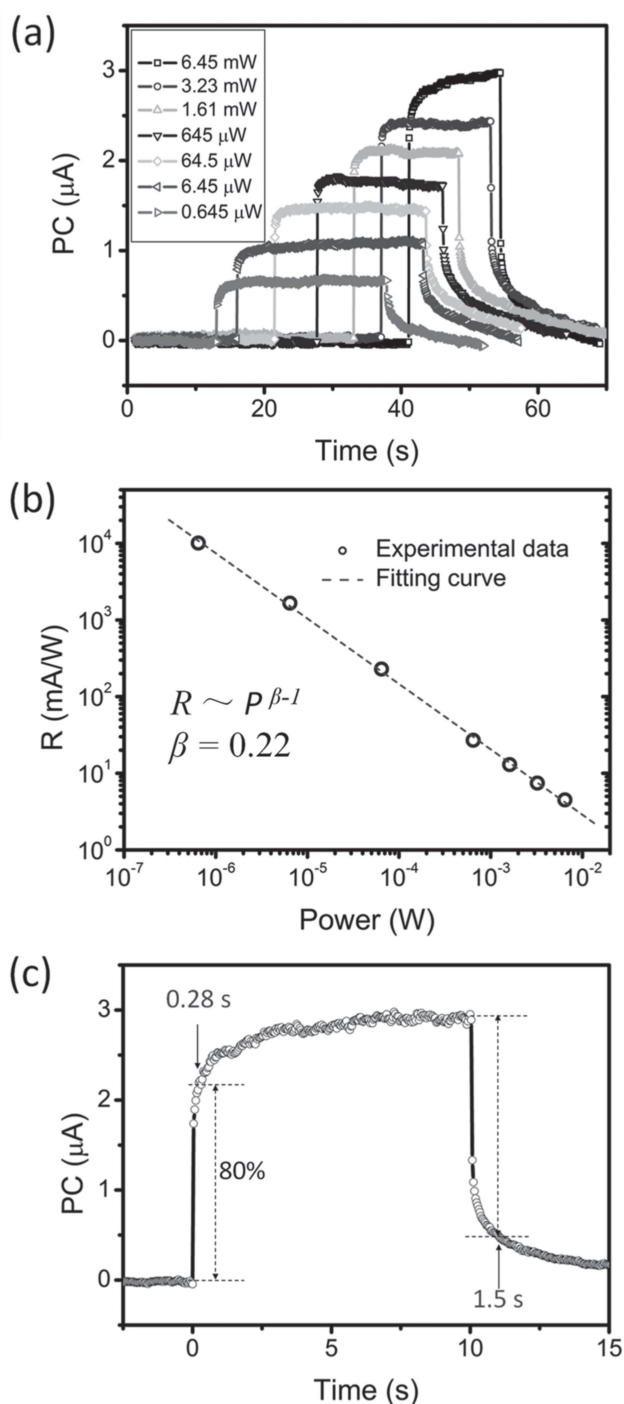

Figure 2. (a) Photocurrent response of a graphene-MoS_2 phototransistor to on-off light irradiation with different light power at a wavelength of 632.8 nm (V_{DS} = 0.1 V; V_{BG} = 0 V). (b) Responsivity as a function of light irradiation power. The dotted line is the best fit to the data using the function $R = \alpha E^{\beta\text{-}1}$, where E is the power of the irradiation light, α and β are constants. (c) Normalized photocurrent response to on/off light irradiation, showing the response rate of the phototransistor.

© 2014 Wiley-VCH Verlag GmbH & Co. KGaA, Weinheim

small NANO MICRO

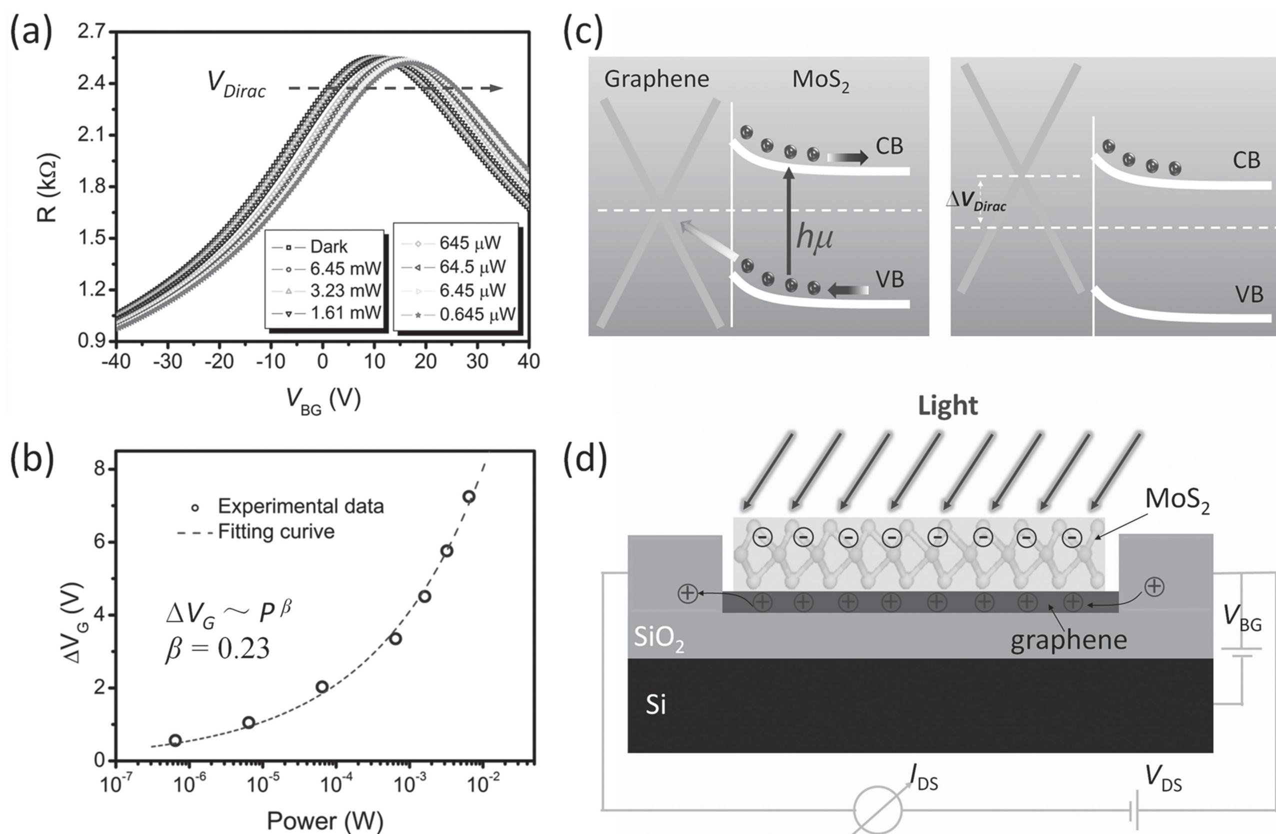

Figure 3. (a) Resistance as a function of back-gate voltage for the graphene–MoS_2 transistor with increasing irradiation power, V_{DS} = 0.1 V. (b) Shift of Dirac point as a function of the optical power illuminating on the graphene-MoS_2 device. (c) Schematic diagram of the charge generation and separation process at graphene/MoS_2 heterojunction under light irradiation. (d) Schematic diagram of the photogating effect of the graphene-MoS_2 phototransistor.

irradiation power reveals a typical Dirac peak with the Dirac point V_{Dirac} (the charge neutrality point) where the resistance is maximum. We could find that the V_{Dirac} shifts to more positive value as the light irradiation power increases, indicating a p-doping effect of graphene. As hypothesized by Dittrich et al.,[30] the photo-excited electron-hole pairs in semiconductor could behave as a Coulomb trap, which can quench the carriers and lead to the decrease of the device conductance and carrier mobility. It is worth pointing out that the transfer curves in our device just show a horizontally positive shift but no any variation in carrier mobility under different irradiation power. Therefore, the response of the phototransistor to light irradiation can be understood by the photogating effect (light modulation of the effective gate voltage applied on the transistor). As shown in Figure 3(c and d), electron-hole pairs (excitons) are generated in the MoS_2 flake under light irradiation and then transfer to graphene film due to the lower energy levels for electrons and holes in graphene. This charge transfer is induced by an internal electric field which arising at the interface due to the workfunction mismatch between graphene and MoS_2 film. In our device, the transfer curves shift to positive gate voltages under light irradiation, indicating that the photo-excited holes transferred into graphene, meanwhile leaving the photo-excited electrons remaining trapped in the MoS_2 film. The negative charges in MoS_2 layer can attract more holes in the graphene film, and thus a higher gate voltage is needed to obtain the Dirac point in the graphene transistor. Increasing the light irradiation leads to a photogating effect enlarged that shifts the Dirac point to even higher back-gate voltage. The shift of the voltage at Dirac point (ΔV_G) of the device as a function of light irradiation power is shown in Figure 3b. The curve can be fitted with the following equation: $\Delta V_G = \alpha E \beta^{-1}$, where E is the power of the irradiation light, α and β are constants and $\beta \approx 0.23$. Benefit from the high mobility of graphene, the transferred photo-excited holes in graphene layer can circulate many times through an external circuit under the driving of bias voltage before it recombines with the photo-excited electrons trapped in MoS_2 layer (Figure 3d), which resulting in the photoresponse gain in our MoS_2-graphene phototransistor. This effect can also be well understood form the equations used for calculating the photocurrent and the responsivity. The photocurrent (PC) of the graphene-MoS_2 phototransistor under light irradiation is given by:

$$\mathrm{PC} = \frac{w c_i \mu \Delta V_G V_{DS}}{L} \tag{1}$$

where C_i is the capacitance of the gate dielectric per unit area, μ is the carrier mobility of graphene, W and L are the width and the length of the channel, respectively.[20] So the responsivity (R) of the device is given by:

 © 2014 Wiley-VCH Verlag GmbH & Co. KGaA, Weinheim

$$R = \frac{PC}{WLE} = \frac{c_i \mu \Delta_G V_{DS}}{L^2 E} \quad (2)$$

The ΔV_G can be considered as the photogate, which is proportional to the quantum efficiency of the device and thus to the light absorption of MoS_2 film. Therefore, the strong absorption of MoS_2 film and the high carrier mobility of graphene ($\approx$2000 cm^2 V^{-1} s^{-1} in our device) which is several orders of magnitude higher than the mobility of a MoS_2 film ($\approx$0.3 cm^2 V^{-1} s^{-1}),[24] are responsible for the ultrahigh responsivity of this phototransistor.

On the basis of the deep understanding of the intrinsic charge transfer mechanism in graphene-MoS_2 phototransistor, it can be further inferred that we should observe both hole current increase and electron-current decrease in the same device using graphene's ambipolar properties. For studying this feature, the device was prepared from mechanical exfoliated graphene which can eliminate the effect of gate hysteresis to the results was used. The transfer curves under light on and off are shown in **Figure 4**a, indicating an obvious positive shift of the V_{Dirac} due to photoinduced p-type doping. Figure 4b shows the time traces of I_{DS} when the same device was held at different gate bias voltages. Similarly, a significant increase of hole current was observed under light irradiation when V_{BG} was held at –20 V, and the photoswitching process was reversible when the light was switched on and off. Remarkably, when V_{BG} was applied at 40 V, we observed, as expected, a fast reversible electron current decrease in the same device under the same irradiation condition. These results are reasonable because photo-excited holes in MoS_2 film can increase the hole current in the p-doping graphene (left inset in Figure 4a) and have an opposing function as the Coulomb traps to scatter (or recombine) the electrons in the n-doping graphene (right inset in Figure 4a). This phenomenon is difficult to be observed in the traditional photoconductor based photodetectors, where just a single carrier conduct, such as MoS_2 or PbS photodetecor. It is worthwhile to emphasize that rational control of the Fermi level of graphene realizes symmetric and opposing photoswitching effects, which are effective for mirror images by using the same graphene-MoS_2 phototransistor.

Figure 4b shows the photocurrent as a function of gate voltage, revealing an obvious gate tunability of the photocurrent response of graphene-MoS_2 phototransistor. The largest responsivity (10^4 mA/W) can be obtained at V_{BG} = –20 V, where the position of graphene Fermi level is at the optimum location for the photo-excited holes to transfer from MoS_2 layer to graphene layer. By tuning the Fermi level close to the Dirac point at V_{BG} = 20 V, the responsivity completely falls to zero. This is because the photo-excited holes are just completely recombined by the electrons from the back gate voltage. Moreover, by tuning the Fermi level far away from the Dirac point at V_{BG} = –60 V, the responsivity also completely falls to zero. This is because the Fermi level of graphene is too low to match with the energy level of MoS_2, and thus the photo-excited holes transfer is forbidden. This feature demonstrates the potential of this device as a gate-tunable phototransistor. This tunability is of great importance in photodetectors because it allows control of the state (on-off) of the detector as well as adjustment of the required gain, depending on the light power to be detected.

Benefit from the recent process in the CVD growth of large area graphene and MoS_2 films,[31,32] large scale, flexible and transparent 2D graphene-MoS_2 hybrid phototransistor was constructed on the polyethylene terephthalate (PET) substrate by using the CVD grown graphene and

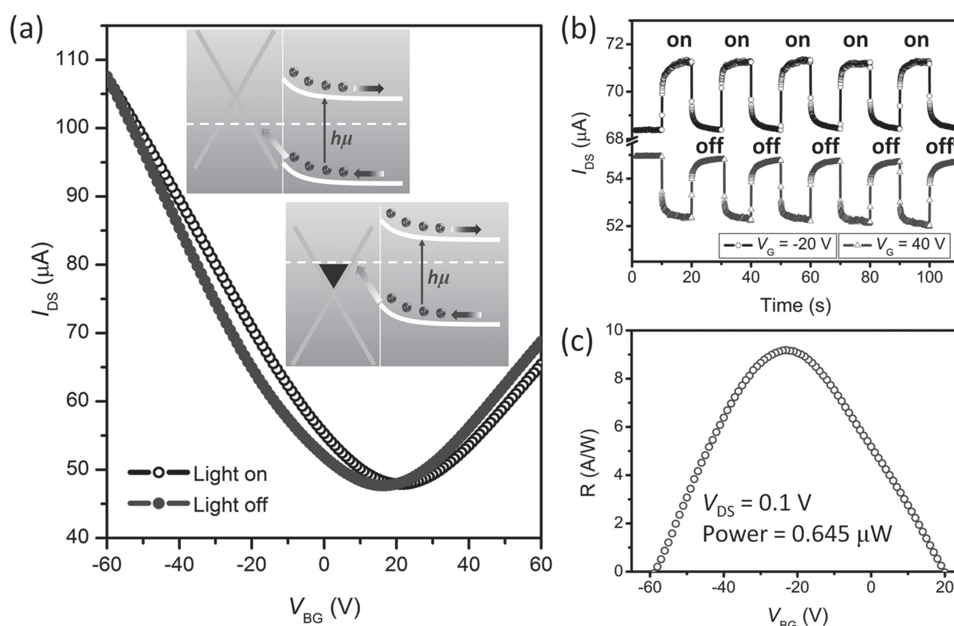

Figure 4. (a) Representative device characteristics of a graphene-MoS_2 transistor under light irradiation and in the dark (V_{DS} = 0.1 V). (b) Time traces of I_{DS} when the device was held at different V_{BG} (V_{DS} = 0.1 V). (c) Responsivity as a function of back-gate voltage, showing that the responsivity of the detector can be directly controlled by the applied back-gate voltage and can be tuned from about 10^4 mA/W (V_{BG} = –23 V) to 0 (V_{BG} = 20 and –60 V) at V_{DS} = 0.1 V.

© 2014 Wiley-VCH Verlag GmbH & Co. KGaA, Weinheim

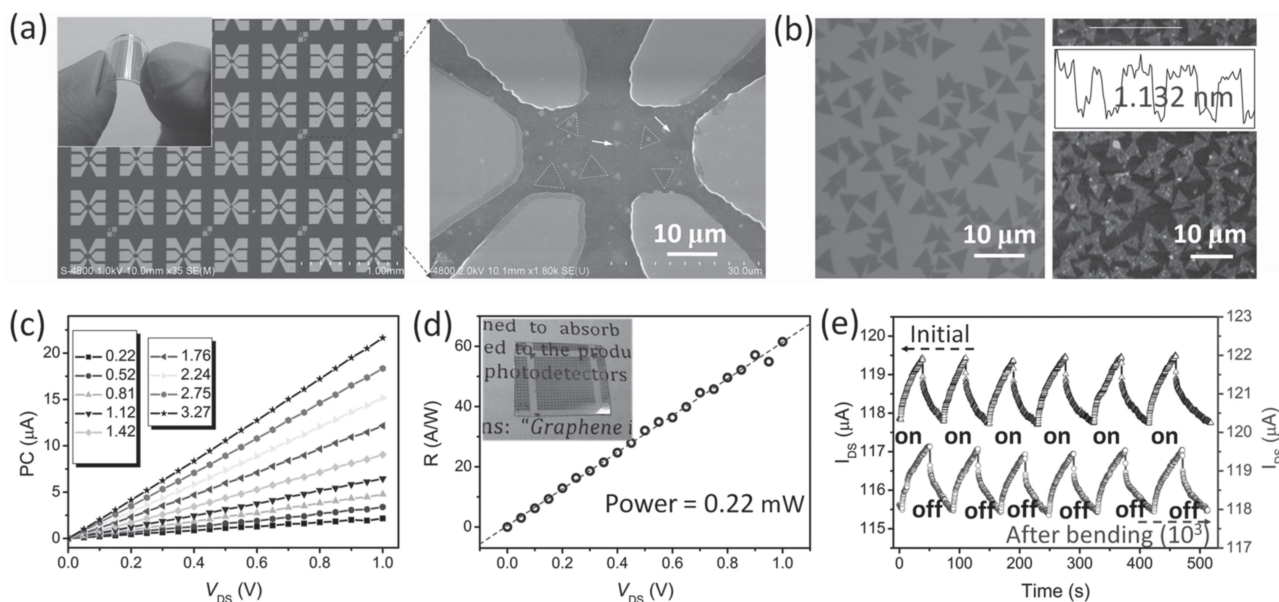

Figure 5. (a) SEM image of a large scale graphene-MoS_2 phototransistor on flexible PET substrate. It is difficuit to clearly observe the profile of graphene film and MoS_2 flakes on PET substrate by using SEM due to the insulation properties of the substrate. The white triangle indicate the MoS_2 flakes in the channel. (b) Optical and AFM images of the CVD grown single layer MoS_2 film on Si/SiO_2 (300 nm) substrate. (c) Photocurrent of the graphene-MoS_2 transistor for different light power as a function of V_{DS}, showing a linear dependence on the bias voltage. The light source is a common whiter light with the intensity being continuously tuned from 0.22 to 3.27 mW/cm^2. (d) Responsivity as a function of the V_{DS} of the device at 0.22 mW/cm^2 light intensity irradiation. (e) Time traces of I_{DS} with the light irradiation on and off of the device measured before (black line) and after (red line) a bending test for about 1000 times (V_{DS} = 0.1 V). Insert on the upper left corner of (a) and (d) are the digital photograph of the phototransistor showing its flexible and transparent features.

MoS_2 films (**Figure 5**a). The same to graphene-MoS_2 phototransistor on SiO_2 substrate, the photocurrent of the phototransistor on PET substrate depends linearly on the V_{DS} and increases with the light irradiation (Figure 5c). As shown in Figure 5d, the responsivity of this phototransistor shows a linearly increase with the V_{DS} increasing, and it can up to 62 A/W with 0.22 mW/cm^2 light intensity irradiation at V_{DS} = 1 V. Figure 5e shows the photocurrent response of the device before and after a bending test for 1000 times. We can find that no obvious degradation be observed in the device after the bending test. As the devices can be easily patterned to small size, large scale arrays of the highly sensitive sensors can be fabricated on flexible substrates for future application in sensing or imaging. It also needs to be noted that the on-off photoswitching effect of the device is much slower than that prepared from mechanical exfoliated graphene-MoS_2 device on SiO_2 substrate. This is because a large amount of electron traps in CVD grown MoS_2 film make the photogererated electrons trapped in the MoS_2 film at the graphene-MoS_2 interface and can't timely recombine with the photogererated holes, and thus lead to the decay of the photocurrent. Fortunately, the response time of this type photodetector can be greatly improved by applying a short gate pulse to discharge the trapped charge carriers.[18] We believe, in the future, increasing the carrier mobility of graphene by improving the graphene quality, or properly prolonging the exciton life-time of MoS_2 film by selective modifying its surface states, can further enhance the responsivity of the graphene-MoS_2 hybrid phototransistor.

3. Conclusion

In summary, based on the idea of implantation of the photoconductance gain, we present a high responsivity 2D graphene-MoS_2 hybrid phototransistor through ingenious combining the advantages of strong light absorption of MoS_2 and the extremely high carrier mobility of graphene. The sensing mechanism is attributed to the photo-excited holes transfer from MoS_2 film to graphene layer under light irradiation, thus increasing the hole carrier current in the p-type graphene and, on the contrary, functioning as Coulomb traps to scatter the electron carriers in the n-doping graphene. It is remarkable that rational utilization of this feature not only acquires a reversible photosensor with fine-tunability and high responsivity, but also realizes mirror-image photoswitching effects in a single device. Our results suggest that through rational complementing the merit and the weakness of two different materials, we could get the effect of "1 + 1>2". We believe that these results provide a deep understanding of interfacial phenomena and offer new attractive insights for building future ultrasensitive devices for applications such as light sensor, optical communication, imaging, memory storage and other multifunction optoelectronics.

4. Experimental Section

Materials: Single layer graphene film was grown on copper foil by using the chemical vapor deposition (CVD) method, and then it was transferred on Si/SiO_2 (300 nm) substrate. Both the

© 2014 Wiley-VCH Verlag GmbH & Co. KGaA, Weinheim

mechanical exfoliated MoS_2 and the CVD grown MoS_2 film were used in our experiment. Few-layers MoS_2 flakes were exfoliated on Si/SiO_2 substrate from the MoS_2 bulk by using scotch-tape based mechanical exfoliation method. The CVD grown MoS_2 film was directly grown on the SiO_2 substrate with the similar method to that previously reported.[33] As shown in Figure 5b, the optical image, AFM image and Raman spectra (Figure S3) show that the CVD grown MoS_2 flakes are single layer. The detailed characterization of the graphene film and MoS_2 flake are shown in Figure S3.

Device Fabrication and Characterization: Graphene-MoS_2 hybrid phototransistor was fabricated by using the following multistep procedure: In typical experiment, first the CVD grown graphene was deposited onto a Si/SiO_2 substrate. Then, the few-layer MoS_2 flake was transferred onto graphene deposited on Si/SiO_2 using the polymer-mediated transfer technique. After that, the contact electrodes Cr/Au (5 nm/50 nm) on graphene were fabricated using standard electron beam lithography and lift-off techniques. Beside, one similar hybrid device was fabricated from the mechanical exfoliated graphene for obtaining more accurate results in Figure 3a,b.

The preparation of the graphene-MoS_2 hybrid phototransistor on the flexible PET substrate is similar to that on the SiO_2 substrate. Briefly, the CVD grown single-layer graphene and the CVD grown MoS_2 films are transferred one after another onto the PET substrate, and then two steps photo lithography were utilized to build the device. The digital photographs and optical image of the flexible device are shown in Figure S4.

The optical and SEM images of the graphene-MoS_2 phototransistor device prepared from the CVD grown graphene and the mechanical exfoliated graphene are shown in Figure S1. The photocurrent measurement was performed on a homemade photoelectric measurement platform which is composed of Horiba HR800 Raman spectrometer and Keithley 4200 semiconductor analyzer. The 632.8 nm laser beam focused by a 50 × objective was used as the incident light.

Supporting Information

Supporting Information is available from the Wiley Online Library or from the author.

Acknowledgement

This work was supported by MOST (2006CB932701, 2006CB932403, 2007CB936203), NSFC (10774006, 50972001, 20725307 and 50821061), "the Fundamental Research Funds for the Central Universities").

[1] G. Konstantatos, E. H. Sargent, *Nat. Nanotechnol.* **2010**, *5*, 391.

[2] P. H. Wobkenberg, J. G. Labram, J.-M. Swiecicki, K. Parkhomenko, D. Sredojevic, J. P. Gisselbrecht, D. M. de Leeuw, D. D. C. Bradley, J. P. Djukic, T. D. Anthopoulos, *J. Mater. Chem.* **2010**, *20*, 3673.

[3] G. Konstantatos, I. Howard, A. Fischer, S. Hoogland, J. Clifford, E. Klem, L. Levina, E. H. Sargent, *Nature* **2006**, *442*, 180.

[4] P. Avouris, M. Freitag, V. Perebeinos, *Nat. Photonics* **2008**, *2*, 341.

[5] A. K. Geim, K. S. Novoselov, *Nat. Mater.* **2007**, *6*, 183.

[6] F. Bonaccorso, Z. Sun, T. Hasan, A. C. Ferrari, *Nat. Photonics* **2010**, *4*, 611.

[7] B. Radisavljevic, A. Radenovic, J. Brivio, V. Giacometti, A. Kis, *Nat. Nanotechnol.* **2011**, *6*, 147.

[8] Z. Y. Zeng, T. Sun, J. X. Zhu, X. Huang, Z. Y. Yin, G. Lu, Z. X. Fan, Q. Y. Yan, H. H. Hng, H. Zhang, *Angew. Chem. Int. Ed.* **2012**, *51*, 9052.

[9] K. G. Zhou, N. N. Mao, H. X. Wang, Y. Peng, H. L. Zhang, *Angew. Chem. Int. Ed.* **2011**, *50*, 10839.

[10] H. Xu, L. M. Xie, H. L. Zhang, J. Zhang, *ACS Nano* **2011**, *5*, 5338.

[11] A. Pospischil, M. Humer, M. M. Furchi, D. Bachmann, R. Guider, T. Fromherz, T. Mueller, *Nat. Photonics* **2013, 7, 851**

[12] K. Yan, D. Wu, H. L. Peng, L. Jin, Q. Fu, X. H. Bao, Z. F. Liu, *Nat Commun* **2012**, *3*, 1280.

[13] T. Mueller, F. N. Xia, P. Avouris, *Nat. Photonics* **2010**, *4*, 297.

[14] D. Basko, *Science* **2011**, *334*, 610.

[15] Z. Y. Fang, Z. Liu, Y. M. Wang, P. M. Ajayan, P. Nordlander, N. J. Halas, *Nano Lett.* **2012**, *12*, 3808.

[16] F. H. L. Koppens, D. E. Chang, F. J. García de Abajo, *Nano Lett* **2011**, *11*, 3370.

[17] M. Furchi, A. Urich, A. Pospischil, G. Lilley, K. Unterrainer, H. Detz, P. Klang, A. M. Andrews, W. Schrenk, G. Strasser, T. Mueller, *Nano Lett.* **2012**, *12*, 2773.

[18] G. Konstantatos, M. Badioli, L. Gaudreau, J. Osmond, M. Bernechea, F. P. G. de Arquer, F. Gatti, F. H. L. Koppens, *Nat. Nanotechnol.* **2012**, *7*, 363.

[19] K. K. Manga, J. Wang, M. Lin, J. Zhang, M. Nesladek, V. Nalla, W. Ji, K. P. Loh, *Adv. Mater.* **2012**, *24*, 1697.

[20] Z. Sun, Z. Liu, J. Li, G. a. Tai, S. P. Lau, F. Yan, *Adv. Mater.* **2012**, *24*, 5878.

[21] H. Wang, L. Yu, Y. H. Lee, Y. M. Shi, A. Hsu, M. L. Chin, L. J. Li, M. Dubey, J. Kong, T. Palacios, *Nano Lett.* **2012**, *12*, 4674.

[22] A. Splendiani, L. Sun, Y. B. Zhang, T. Li, J. Kim, C. Y. Chim, G. Galli, F. Wang, *Nano Lett.* **2010**, *10*, 1271.

[23] T. Cao, G. Wang, W. P. Han, H. Ye, C. R. Zhu, J. R. Shi, Q. Niu, P. H. Tan, E. Wang, B. L. Liu, J. Feng, *Nat Commun* **2012**, *3*, 887.

[24] H. S. Lee, S. W. Min, Y. G. Chang, M. K. Park, T. Nam, H. Kim, J. H. Kim, S. Ryu, S. Im, *Nano Lett.* **2012**, *12*, 3695.

[25] Z. Y. Yin, H. Li, H. Li, L. Jiang, Y. M. Shi, Y. H. Sun, G. Lu, Q. Zhang, X. D. Chen, H. Zhang, *ACS Nano* **2011**, *6*, 74.

[26] W. Choi, M. Y. Cho, A. Konar, J. H. Lee, G. B. Cha, S. C. Hong, S. Kim, J. Kim, D. Jena, J. Joo, S. Kim, *Adv. Mater.* **2012**, *24*, 5832.

[27] L. Xu, X. Zhou, Y. Yu, W. Q. Tian, J. Ma, S. Lei, *ACS Nano* **2013**, *7*, 8066.

[28] L. Britnell, R. M. Ribeiro, A. Eckmann, R. Jalil, B. D. Belle, A. Mishchenko, Y. J. Kim, R. V. Gorbachev, T. Georgiou, S. V. Morozov, A. N. Grigorenko, A. K. Geim, C. Casiraghi, A. H. C. Neto, K. S. Novoselov, *Science* **2013**, *340*, 1311.

[29] H. Xu, J. X. Wu, Y. B. Chen, H. L. Zhang, J. Zhang, *Chem. Asian J.* **2013**, *8*, 2446.

[30] T. Dittrich, V. Duzhko, F. Koch, V. Kytin, J. Rappich, *Phys. Rev. B* **2002**, *65*, 155319.

[31] X. S. Li, W. W. Cai, J. An, S. Kim, J. Nah, D. X. Yang, R. Piner, A. Velamakanni, I. Jung, E. Tutuc, S. K. Banerjee, L. Colombo, R. S. Ruoff, *Science* **2009**, *324*, 1312.

[32] K. K. Liu, W. J. Zhang, Y. H. Lee, Y. C. Lin, M. T. Chang, C. Y. Su, C. S. Chang, H. Li, Y. M. Shi, H. Zhang, C. S. Lai, L. J. Li, *Nano Lett.* **2012**, *12*, 1538.

[33] S. F. Wu, C. M. Huang, G. Aivazian, J. S. Ross, D. H. Cobden, X. D. Xu, *ACS Nano* **2013**, *7*, 2768.

Received: November 27, 2013
Revised: January 10, 2014
Published online: March 24, 2014

© 2014 Wiley-VCH Verlag GmbH & Co. KGaA, Weinheim